ORCA – Online Research @ Cardiff

A New Insight into Modeling Passive Suspension Real Test Rig System with Considering Nonlinear Friction Forces

Ali Al-Zughaibi   Yiqin Xue   Roger Grosvenor

Abstract

A major purpose of any vehicle suspension system is to isolate the body from roadway unevenness disturbances. Although the limitation of passive suspension, it is still continuously improved and to use the available suspension deflection to provide maximum isolation. In most research works reported earlier, in contrast to the real suspension system, the quarter car was modeling as vertically moved of viscose damper and stiffness spring (VD & SS). The motivation for the present study that focuses on reality situation. In order to take into account the actual configuration of test rig system, a new passive suspension system model with implementing the nonlinear lubricant friction forces that effected at the linear bearing body, the friction model will be captured most of the friction behavior that has been observed experimentally, will be considered. On the other hand, an active actuator is used to generate the inputs system as a road simulator therefore, a nonlinear hydraulic actuator model included the dynamic of servovalve derived by the proportional-integral (PI) controller will be prepared. This study is achieved experimentally and simulation using C++ compiler. As results, a good agreement between the experiment and simulation results is obtained i.e. the passive suspension system with considering nonlinear friction and the nonlinear hydraulic actuator with servovalve equation models are quite accurate and usefulness. The PI controller is suggested successfully derived the hydraulic actuator to valid the control scheme. The ride comfort and handling response are closed to what respected for the passive suspension system.

Keyword passive suspension, non-linear hydraulic actuator, dynamic servovalve, PI control.

NOTATION

A_{1r}	Actuator cross-sectional area for side1 = 1.96e-3(m^2)	M_T	Total mass = 285 (kg)
A_{2r}	Actuator cross-sectional area for side2 = 0.94e-3(m^2)	M_b	Body mass = 240 (kg)
β_{re}	Effective bulk modulus =1.43e9 (N/ m^2)	M_r	Tyre mass = 5 (kg)
b_d	Viscous damping = 260 (N/m. s^{-1})	M_w	Wheel mass = 40 (kg
b_t	Tyre damping = 3886 (N/m. s^{-1})	k_t	Tyre stiffness = 9.2e5 (N/m)
B_{vr}	Actuator viscous damping = 500 (N/m. s^{-1})		
L_d	Free length of viscous damper = 0.342 (m)	k_s	spring stiffness = 2.89e4 (N/m)
R_{ir}	Internal leakage resistance=2.45e11 (N/ m^2/m)	P_{sr}	Supply pressure = 200e5 (N/ m^2)
K_{fr}	Servovalve flow constant = 0.99e-4 (m^3. s^{-1}/mA)	Q1r, Q2r	Flow rates (l/min)
V_{1r0}	Actuator volume for side 2=80e-6 (m^3)	P_{1r}, P_{2r}	Pressures (N/ m^2)
V_{2r0}	Actuator volume for side 1=167e-6 (m^3)	τ_r	Time servovalve constant (s)

Al-Zughaibi Ali was a lecturer with Engineering College, University of Karbala, Iraq. He is currently a PhD student at Cardiff School of Engineering, Cardiff University, Cardiff, UK, (Email: Al-ZughaibiAI@cardiff.ac.uk).

Xue Yiqin is with the Cardiff School of Engineering, Cardiff University, Cardiff, UK, (Email: Xue@cardiff.ac.uk)

Grosvenor Roger is with the Cardiff School of Engineering, Cardiff University, Cardiff, UK, (Email: Grosvenor@cardiff.ac.uk)

1   Introduction

Suspension system isolates a vehicle body from road irregularities in order to maximise passenger ride comfort and retains continuous road-wheel contact to provide road-holding, (Hedrick and Butsuen 1990). Traditionally, automotive suspension designs have been a compromise between the three conflicting criteria of passenger comfort road, suspension travel and road holding, which are also called as design goals. Good ride comfort requires a soft suspension, whereas insensitivity to applied loads requires stiff suspension. Electronically controlled suspension systems can potentially improve the ride comfort as well as the road handling of the vehicle (Hrovat 1997). Road handling relates patch contact load between the tyres and road surface and related to tyre displacement and suspension travel. In a passive system, parameters are specified, being to achieve a certain level of compromise between road holding, load carrying, and comfort. The passive suspension system is an open loop control system, which only designs to achieve certain condition only. Because of the characteristic of this system were fixed and cannot be adjusted by any mechanical part. Therefore, the performance of the passive suspension depends on the road profile. The traditional passive suspension system design is carried out by attempting to meet design demands through various optimization methods.

Quarter car model can successfully be used to analyse the suspension system responses to road inputs but accuracy of the results obtained will depend on how accurately and effectively the system parameters have been measured (sprung mass, unsprung mass, stiffness, and damping), the system responses with different road excitations can be obtained (Pathare 2014) and the model establishing.

Electro-hydraulic servo systems (EHSS) are widely used in many industrial applications and mobile systems because of their high power-to-weight ratio, high stiffness, fast response, self-cooling, good positioning capabilities, etc. However, the dynamical models of the EHSS have many uncertainties, which are consequences of physical characteristics, disturbances and load variations (FitzSimons and Palazzolo 1996). The dynamic behaviour of these systems is highly nonlinear due to the phenomenon such as pressure-flow characteristics, hysteresis in flow gain characteristics, oil leakage, oil temperature variations, characteristics of valves near null, and so on. In practice, determining the exact dynamic model that will contain all the physical phenomena of EHSS represents a difficult task. The dynamics of hydraulic systems are highly nonlinear (Merritt 1967). (Maneetham and Afzulpurkar 2010) presented a proportional derivative controller for high-speed nonlinear hydraulic servo system. (Alleyne and Hedrick 1995) considered the nonlinear dynamics of an electro-hydraulic actuator in a quarter car active suspension model and used these dynamics to formulate a nonlinear control law.

Most of the earlier researchers, (Hanafi et al. 2009), (Jamei et al. 2000), (Tan and Bradshaw 1997), (Westwick et al. 1999), (Buckner et al. 2015), and (Hardier 1998), a quarter car modeling is generally assumed that the VD & SS are moved vertically, with ignored the inclination effects. In contrast, in the real word they mostly inclined, therefore there is no apriori reason to make this assumption now. In addition, when we tried to use the vertical model to simulate the passive suspension test rig, which already existed at Cardiff University and is shown as a picture in Fig.1 and as a schematic diagram in Fig. 2, we faced an issue, there is a significant different between body travel at experimental and simulation results. Since we should modify the test rig suspension model, to take into account the actual organisation of VD & SS systems, therefore, the nonlinear friction

3

forces that effected at linear bearing body will be played a pivotal role to reduce body oscillation, should be considered.

In the current study, modeling of a nonlinear hydraulic actuator with executing the dynamic servovalve derived by PI controller, proposing a paradigm passive suspension system model with implementing friction forces, for the test rig will be conducted. Experimental work and simulation will be accomplished as a function to amendment into step input (SI) parameter, to check the availability of these models from one hand, and to study the ride comfort and road handling although present limitation of the passive suspension system with the road disturbance on the other hand.

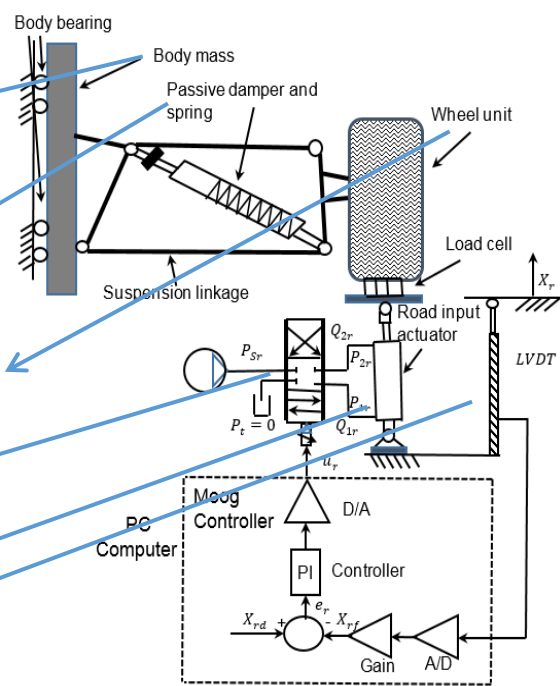Fig. 1 Photograph of the test rig

Fig. 2 Schematic diagram of test rig and road

The organisation of this paper is, in section 2, we state the dynamic nonlinear hydraulic road actuator include servovalve equation model with a short summary about PI controller. Section 3 showed the new passive suspension system model with more detail

4

about the nonlinear friction models. While the identification parameters are specified in section 4. However, the experimental and simulation results are evidently showing and discussing in section 5. Finally, section 6 point out the main results and a direction to expand the current results and recommendations for future work.

2   Road simulator model

The road simulator system was designed in order to generate step and sine wave road input to the passive system. Step input will be used; that could be because it is help to easy show the responses within the input variations, also it is impossible to directly give steps input since it should be moved the piston to mid-point of the hydraulic actuator, therefore the input to the system are mixed between the ramp and step input. For step input, we will pass it across the filter to avoid test rig damage. Displacement and velocity outputs of the road simulator system become disturbance inputs for the passive suspension system. Therefore, this system is dynamically related and the dynamic behaviour of the road simulator system becomes an important factor in this study, and ought to be investigated.

The piston is assumed to be supporting a vertical load acting such that it always attempts to retract the piston, that is, it always acts in the same direction. For open-loop control systems, a critically lapped servovalve spool is assumed, and for closed-loop control systems, asymmetrically underlapped servovalve spool is always assumed. The latter assumption is more useful for closed-loop analysis since a small amount of spool underlap often occurs in practice (Surawattanawan 2000). It is also an easy matter to reduce the underlap to zero to simulate a critically lapped spool, should this be desirable. The servovalve flow equations and the nonlinear hydraulic actuator dynamic may be written as follows:

2.1 Mathematical modeling

The modeling of a single rod actuator under closed loop position control, PI controller, with known actuator seal leakage presents interesting variations from the usually published literature. It will be shown theoretically that this system results in three position offsets due to; The seal leakage term, the "integrator removal" characteristic by the "hypothetical" open loop transfer function, and the dynamic equation of servovalve.

Considering Fig. 2, road simulator schematic diagram and the conventional modeling (Alleyne and Hedrick 1995) and (Watton 2007). The spool valve displacement x_{sr} is related to the voltage input u_r by a first order system gave by:

$$\dot{x}_{sr} = \frac{1}{\tau_r}(u_r - x_{sr}) \tag{1}$$

Therefore, depending on the direction of servovalve spool movement we have two cases:

Case1: for $x_{sr} \geq 0$ when extending

The flow rates equations are:

$$Q_{1r} = K_{fr}\, x_{sr}\sqrt{|P_{sr} - P_{1r}|}\; sign(P_{sr} - P_{1r}) \tag{2}$$

$$Q_{2r} = K_{fr}\, x_{sr}\sqrt{|P_{2r}|}\; sign(P_{2r}) \tag{3}$$

Case 2: for $x_{sr} < 0$ when retracting

The flow rates equations are:

$$Q_{2r} = K_{fr}\, x_{sr}\sqrt{|P_{sr} - P_{2r}|}\; sign(P_{sr} - P_{2r}) \tag{4}$$

$$Q_{1r} = K_{fr}\, x_{sr}\sqrt{|P_{1r}|}\; sign(P_{1r}) \tag{5}$$

The actuator flow rate equations, including compressibility and cross-line leakage effects for both sides, may be written.

$$\frac{V_{1r}}{\beta_r} \, \dot{P}_{1r} = Q_{1r} - A_{1r}\dot{X}_r - \frac{(P_{1r}-P_{2r})}{R_{ir}} \tag{6}$$

$$\frac{V_{2r}}{\beta_r} \, \dot{P}_{2r} = A_{2r}\dot{X}_r + \frac{(P_{1r}-P_{2r})}{R_{ir}} - Q_{2r} \tag{7}$$

In addition, the 2nd Newton law for mass tyre is,

$$\ddot{X}_r M_r = (P_{1r}A_{1r} - P_{2r}A_{2r} - B_{vr}\dot{X}_r - k_t(X_r - X_w) - B_t(\dot{X}_r - \dot{X}_w) - M_T * g \tag{8}$$

A low voltage is used to control the servovalve. The control voltage is passed through an amplifier, which provides the power to alter the valve's position. The valve will then deliver a measured amount of fluid power to an actuator in a similar way that shown in (Kirk). The use of a feedback transducer on the actuator returns an electrical signal to the amplifier to condition the strength of the voltage to the servovalve. The main drawback of state feedback law (static-state controller), is that it cannot eliminates the steady-state errors due to hydraulic leakages and constant disturbances or reference input commands. To remove this drawback, it is necessary to consider the controller structure that contains an integral action.

The controller to be suggested is:

$$u_r = K_p * e + K_i * e * Ts \qquad \text{[PI controller]} \tag{9}$$

$$e = X_{rd} - X_{rf} \tag{10}$$

Note: For more detail, see APPENDIX.

3   New passive suspension system model

Vehicle suspension systems have developed over the last 135 years to a very high level of sophistication. Most manufacturers today use a passive suspension system employing some type of springs in combination with hydraulic or pneumatic shock absorbers. Despite the wide range of designs currently available, passive suspensions, because they can only store and dissipate energy in a pre-determined manner, will always be a compromise between passenger ride comfort, handling, and suspension stroke over the operating range.

To understand the characteristic of a passive suspension, it is theoretically investigated and designed using the suspension working space from the quarter car test rig. This is based on a practical viewpoint that a suspension designer must optimise the system within the limited working space. Therefore, this model should be to take into account the actual organisation of VD & SS systems, i.e. the friction force that effected on bearings, should be specified due to the inclination dynamic angle ($\theta \mp \Delta\theta$). The mass plate used to represent a quarter car body is constrained to move vertically via two linear bearings, two rails (THK type HSR 35CA), 1000 mm long and parallel to each other, are used with each linear bearing.

Considering the free body diagrams of both body and wheel masses as shown in Fig. 3. A quarter car model of a passively suspended vehicle, where M_b and M_w are the masses of the body and wheel respectively. The wheel and car body displacements are X_w, X_b respectively. The spring coefficients for system and tyre are k_s and k_t. The damper coefficient for body and tyre are b_d and b_t. θ is the construction angle. It should be noted that X_r, X_w and X_b are mathematically referenced with an ideal ground, which does not exist in real world, but does exist in the laboratory environment.

3.1 Nonlinear friction forces model

In this study, we will consider the real inclined position for the VD & SS; therefore, the normal load applied to the body mass should be assessment, which is responsible for generating the bearings friction forces. However, we will reflect how to calculate these friction forces in the following analysis with assumed the linkage as one member. The past few decades have witnessed an increasing preoccupation with friction modeling for the purpose of understanding, simulation, and control in a variety of disciplines ranging from geophysics to electromechanical systems. (Armstrong-Hélouvry et al. 1994) has surveyed on friction in general mechanical systems and gave a detailed analysis of many models available including the work done by (Karnopp 1985). In Kamopp's friction velocity model, a section with a width of small distance near zero velocity was defined to restrain any motion until certain forces, were exerted on the system. This model was extended works on basic stiction-coulomb friction model. Dahl's model as studied by (Bliman 1992)*,* however, move beyond previous stick-slip model to include a hysteresis loop and describes various steps for formulating a mathematical model of the hysteresis loop. There are numerous other works done to describe the hysteresis motion and its modeling ranges from simple gain model to a model that includes hysteresis loop in their model. The successful design and analysis of friction compensators depend heavily upon the quality of the friction model used, and the suitability of the analysis technique employed. Friction is a natural phenomenon that is quite hard to model, and it is not yet completely understood, which is a dominant nonlinear factor that seriously deteriorates positioning accuracy of the suspension system model.

In practice, it is not possible to determine an exact friction model, however; based on observed measurement results, a new friction model is developed. The model includes a stiction effect, a linear term (Viscous friction), a non-linear term (Coulomb friction), which is depend on the dynamic normal force but whose sign depends on the direction of

body velocity, and an extra component at low velocities (Stribeck effect). During acceleration, the magnitude of the frictional force at just after zero velocity be dipped due to Stribeck effect which means the influence of a friction decrease from direct contact of bearings and body into the mixed lubrication mode at low velocity, this is could be due to lubricant film behaved.

The mathematical expression for the new friction model is complicated with consisting different terms, which are built to accurately represent the observed phenomena, with physical insight gets sensible in such cases as shown in (11).

$$F_{fric} = \begin{cases} 0.0 & \text{data acqustion delay} \\ k_s(X_w - X_b) + b_d(\dot{X}_w - \dot{X}_b) & \dot{X}_b = 0.0 \\ C_e * e^{(\dot{X}_b/e1)} - \left[\frac{\mu*(k_s*(X_w-X_b)+ b_d*(\dot{X}_w-\dot{X}_b))}{\tan(\theta \mp \Delta\theta)}\right] + D * \dot{X}_b & \dot{X}_b > 0.0 \\ -C_e * e^{(\dot{X}_b/-e1)} - \left[\frac{\mu*(k_s*(X_w-X_b)+ b_d*(\dot{X}_w-\dot{X}_b))}{\tan(\theta \mp \Delta\theta)}\right] + D * \dot{X}_b & \dot{X}_b < 0.0 \end{cases} \quad (11)$$

This model, which has now become well established, has been able to give a more satisfactory explanation to observed dynamics fluctuation of body mass. It will be tried heuristically to ''fit'' a dynamic model to experimentally observed results. The resulting model is not only quite valid for our test rig behaviour, which can provide evidently a physical explanation, but also is reasonably suitable for most general cases. In addition, it has able to consider the facets of low-velocity friction force dynamics (that we are aware of), with involving arbitrary steady state friction characteristics. Because of the test rig schematic and the system input signal, which with a history travel, therefore, we have three circumstances depending on whether the body velocity is accelerating or decelerating at positive or negative direction.

Equation (11) show the friction model, which includes two main parts of frictions: Static and dynamic frictions with two expressions depend on the velocity direction, we will give a summary for each of the following:

The static friction, the stiction area, is solely dependent on the velocity that could be because the body velocity is close to zero or just across zero often. The static models counted from the test rig forces balance ($\sum F_v = 0.0$), at beginning test time, whereas the wheel is started to move as relative to the road inputs, the body remain at motionless ($\dot{X}_b = 0.0$), that be accurately enough to describe the stiction region. As shown in (11) by:

$$F_{fricS} = [k_s(X_w - X_b) + b_d(\dot{X}_w - \dot{X}_b)] \tag{12}$$

Where, F_{fricS} is static friction, which is a function of the relative displacement and relative velocity between the wheel and body multiplies by SS & VD respectively, with direction totally depending on the next stage $\dot{X}_b$ direction. In another word, pre-sliding displacement, which exhibits that friction characteristics like a spring, when the applied force is less than the static friction breakaway force. From experiment work, we found that the maximum stick friction force occurs occasionally when $(X_w - X_b) \leq$ 0.0069 m & $X_b \cong 0.0$. At the same time, this friction will be description the steady state friction characteristics with everywhere happen.

While, the dynamic model is necessary, which introduces an extra state at positive and negative values depend on the sign $\dot{X}_b$ as shown in (11), which can be regarded as to: first, the Transition behavior from stiction to slid regime includes the Stribeck effect with C_e is tracking parameter, and e1, is the degree of curvature. Second, the Colombo friction resulting relative to the normal dynamic force at body bearing, with suitable friction coefficient (μ). Third, the Viscous friction will depend on velocity and suitable viscous coefficient (D). The most crucial results of this model are highlight clearly the hysteresis behaviours of friction relative to body displacement and velocity behaves history.

3.2 How to account the normal force

In the following, we will explain how to account the normal force at bearing body, which will be responsible for generating Colombo friction, by drawing the free body diagram of the test rig as will show in Fig. 3.
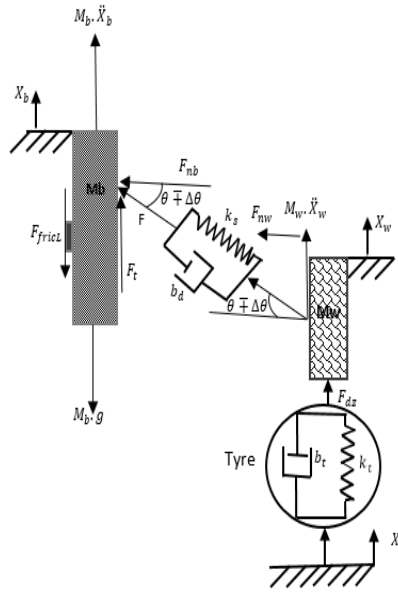

Fig. 3 Free body diagram of test

The normal force be acted at lubricant bearings body is

$$F_{fric} = \left[\frac{\mu*(k_s*(X_w-X_b)+ b_d*(\dot{X}_w-\dot{X}_b)}{\tan(\theta \mp \Delta\theta)} \right]$$ (13)

In addition, the dynamical construction linkage angle will be changed as $\mp\Delta\theta$, and from the geometric analysis as shown in APPENDIX, we will find:

$$\Delta\theta = \sin^{-1}\left[\frac{(X_w-X_b)*\sin(\theta)}{L_d-(X_w-X_b)*\sin(\theta)} \right]$$ (14)

Where, L_d is the free length of VD & SS.

Note: For more detail, see APPENDIX.

3.3 Passive mathematical model

Vehicle suspensions are designed to minimise the car body acceleration $\ddot{X}_b$ within the limitation of the suspension displacement $X_w - X_b$ and tyre deflection $X_r - X_w$. Hence, these three vehicle response variables, that should be examined.

(Surawattanawan 2000) was conducted a study for same test rig within the lack of consideration the real position for VD & SS, as result, he ignored the friction affects. We are first researchers will implementing the friction forces within the Newton 2nd law for a quarter car model, therefore, considering Fig. 3, the new dynamic equation of motion for the mass body passive system becomes:

$$M_b.\ddot{X}_b = [k_s(X_w - X_b) + b_d(\dot{X}_w - \dot{X}_b)] - F_{fric} \tag{15}$$

While, the dynamic equation of motion for the mass wheel is:

$$M_w.\ddot{X}_w = -[k_s(X_w - X_b) + b_d(\dot{X}_w - \dot{X}_b)] + k_t(X_r - X_w) + b_t(\dot{X}_r - \dot{X}_w) \tag{16}$$

4 Parameters identification

According to the mathematical model of the passive suspension system and the road simulator developed in this paper, the parameters that may be identified are as follows:

Spring stiffness k_s, viscous damping b_d, tyre stiffness k_t, tyre viscous damping b_t, actuator viscous damping B_{vr}, effective bulk modulus β_{re}, and cross-port leakage resistance R_{ir}.

The four parameters [k_s, b_d, k_t, and b_t], could be directly valid from the experiment test data by applying the Newton 2nd law for body and wheel masses separately as shown in

13

(15) and (16). We have to use test data to find the accelerations for body and wheel masses, to obtain these parameters values one-to-one.

To identify β_{re}, which be measured of the compressibility of the fluid and is inevitably required to calculate hydraulic undamped natural frequencies in a system. It is perhaps, the one fluid parameters cause most concern in its numerical evaluation due to other effects. To elaborate how to measure the β_{re}? The road servovalve has two lines, the upper one is a steel pipe, there is a formula to calculate the effective bulk modulus as mentioned at (Watton 2009). While the bottom line is mixed from a steel and hosepipe, in contrast, for hose it very complex to calculate it. (Watton 2009) was conducted hose effective bulk modulus values by experiment test, in the author opinion, is suitable to use this value and compared it with that of steel pipe, the latter is dominated, therefore, we will use β_{re} of steel pipe for both lines in our test.

While the others two parameters [B_{vr} and R_{ir}], we smoothly can use the value from (Surawattanawan 2000), the author had already identified for the same test rig.

5   Experimental and simulation results

To doing experiment test, serial processes should be made before starting the experiment work. This come from to make sure, sensors be used to measure signals such as displacement (LVDT), velocity (WGS2) for road, wheel and body, also that be used to measure pressures and flow rates of servovalve, the Moog servo-valve (type E671, 20 l/min rated flow, 100 mA rated current), for road simulator, correctly work and to calibrate them as well. In addition, a control program is designed to control the SI to the system.

In this study, comparatives results are collected from the experiment works, for different parameters such as displacements and velocities for road, wheel, and body, also the

relative displacement between wheel and body, with that results are achieved from a simulation, through C++ compiler. These results are gained by varying SI parameter, it could be vital for the current study, which has been changed into three amplitude values (70, 50 and 30 mm), the distance between the mid-point to top-point of the actuator.

The experimental and simulation results are displayed in two columns, left one representing the experimental results in compared with a right column that shows the simulation results, according to the values of SI, although we are conducting three experimental cases but we will just show one case for (SI = 50 mm) as following:

Fig. 4 shows comparisons between experimental and simulation results for actual SI, road simulator input, the original one (Xrd), is mixed between the ramp and step inputs with $\mp$50 mm amplitude, this signal will be passed through first order filter to be more convenient with the test rig, to avoid damage, and the real input measured X_r. It is clearly seen that there are quite similar between these inputs at experiment and simulation and that what we respected to make a good comparing them. Fig. 5 is demonstrated two signals, the former is the error signal between the desired and measured road displacement. It is clearly seen that there is a small steady state error, a possible explanation for this might be that is the cross leakage between two actuator chambers from this reason we considered the integral controller, whilst the latter figure shows the proposed controller, PI controller, that be used to derive the system from achieving his target. Fig. 6 displays the top and bottom pressures of road actuator. While Fig. 7 shows a comparison between experimental and simulation results for wheel and body displacement. It is clearly seen that there is a delay for body travel compare with wheel travel at begging, this is because of the static bearing friction forces, in general, they are identical behaviour between both and they be traveled flowing the road simulator with showing the friction effects. Fig. 8 shows the experimental and simulation results for wheel velocity with a good agreement for both. It is observed that there is a slim

difference in values, the simulation values higher than the experiment values, thus is might be because considering a linear suspension model. While, Fig 9 displays the experimental and simulation results for body velocity with a worthy agreement for both, and this comparing one of the two signals are helped at validation friction. In general, the experimental results with extremely noises that might be because of sensitive's sensor. Forasmuch, Fig. 10 shows the difference between wheel and body displacement ($X_w - X_b$) in (m) for experimental in compared with simulation results. It is important to display this difference in order to know the allowance or might be to find the weather condition of the test rig. In addition, this relative displacement has direct link close to the relation with real word situation. From Fig. 10, it is clearly seen that at the beginning test time, there are high differences between the wheel and body travels. That could be relative to the static friction force, stiction region, while the wheel start to move the body motionless ($\dot{X}_b = 0.0$), then the total forces be greater than threshold force i.e.($\dot{X}_b > 0.0$), since the difference gradually decreases until reach the second SS cases, it shows the nonlinear Stribeck effects and the late behaviours relative to dynamic friction. This signal will successfully help to make a physical explanation for the observation friction phenomena.

However, Fig.11 has demonstrated the total nonlinear friction as a function of body velocity. The test rig schematic and the system inputs signal that with a history travel helps to generate the hysteresis friction behaviours. This depending on whether the body velocity is accelerating or decelerating, the velocity values be started from zero and just after velocity reversals be reached the highest and will be backed to zero or close to zero at SS. Therefore, from Fig. 11, it is clearly seen that at $\dot{X}_b = 0.0$, the stiction area, the friction is equal to static friction as shown in system (11). Then at just cross $\dot{X}_b = 0.0$, the friction directly dips relative to Stribeck effect, this is could be because the hydraulic layer behave. After that $\dot{X}_b > 0.0$, it will be drawn two hysteresis loops in a positive

direction, while $\dot{X}_b < 0.0$, it also helps to generate a hysteresis loop in an opposite direction with a twice values that because the velocity value is double.
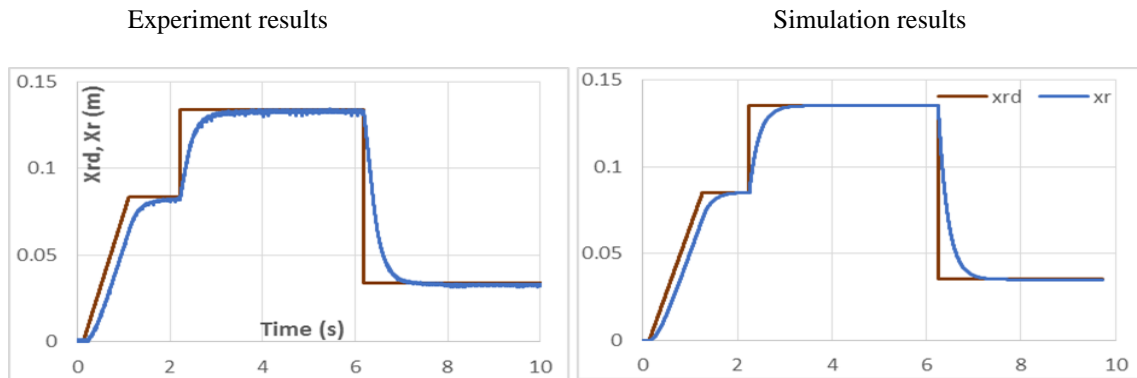
Experiment results   Simulation results

Fig. 4 Comparing of step input X_{rd}, X_r (m), experiment and simulation ($X_r=\mp0.05$ m, road input)
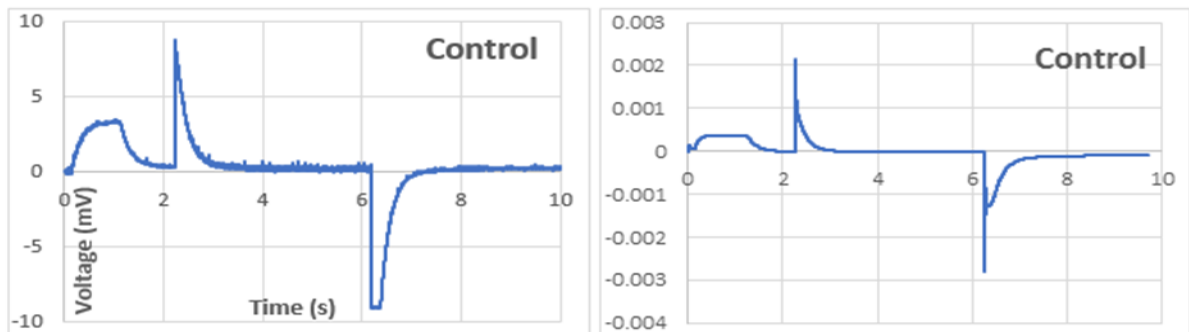
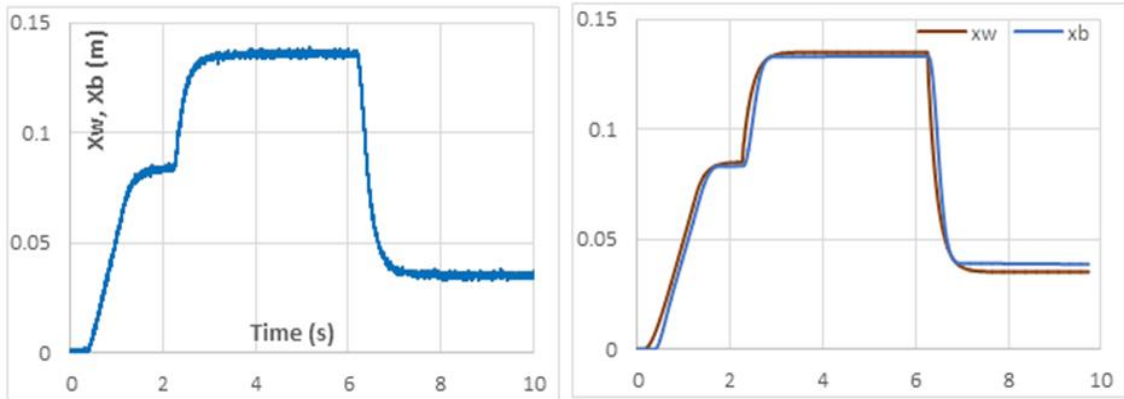Fig. 5 Comparing Control force supposed to be the system
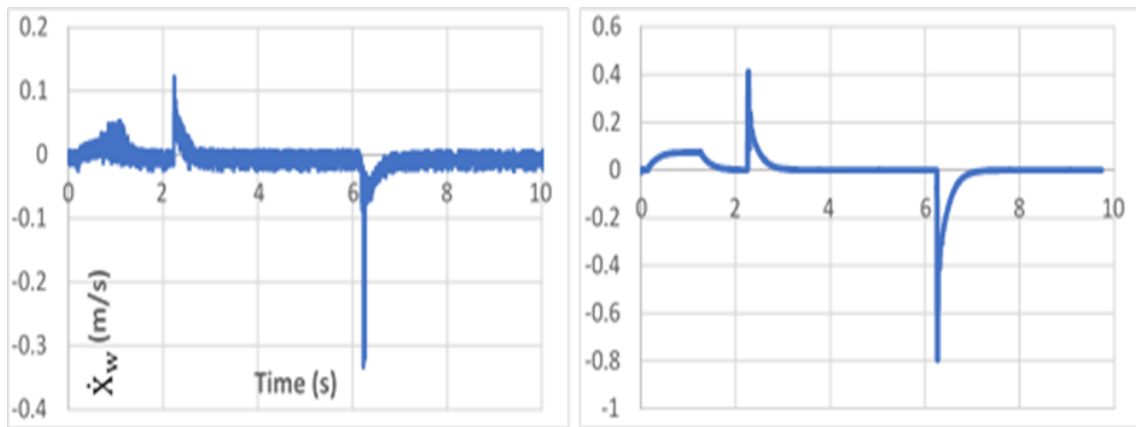
Fig 7 Comparing of X_w, X_b (m),

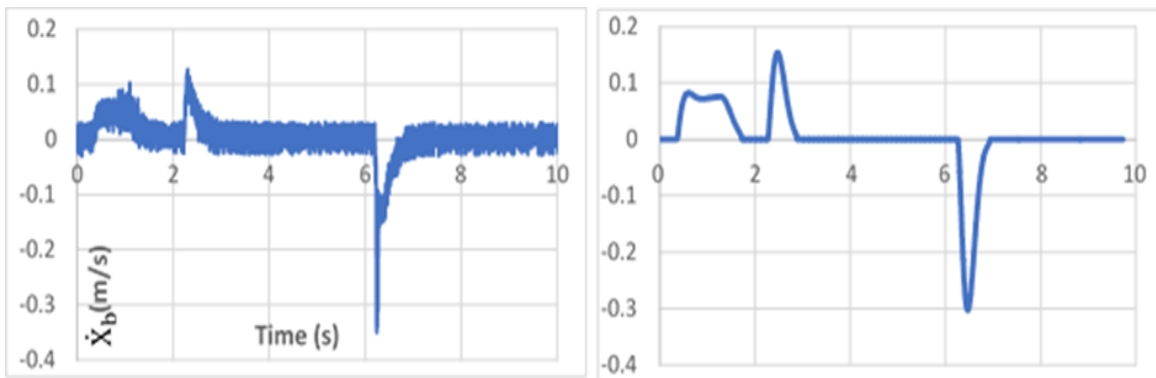Fig. 8 Comparing between $\dot{X}_w$ (m/s), ($\dot{X}_w$, wheel velocity)

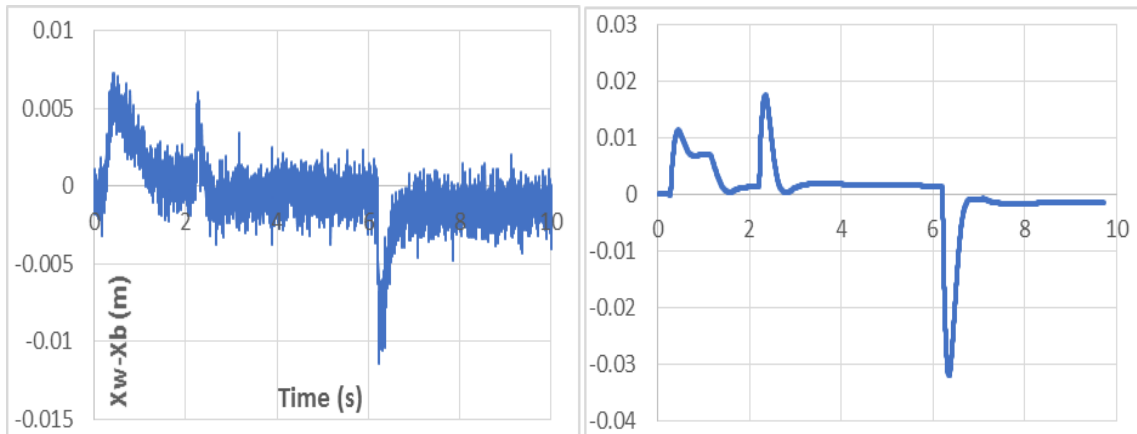Fig. 9 Comparing between $\dot{X}_b$ (m/s), ($\dot{X}_b$, body velocity)

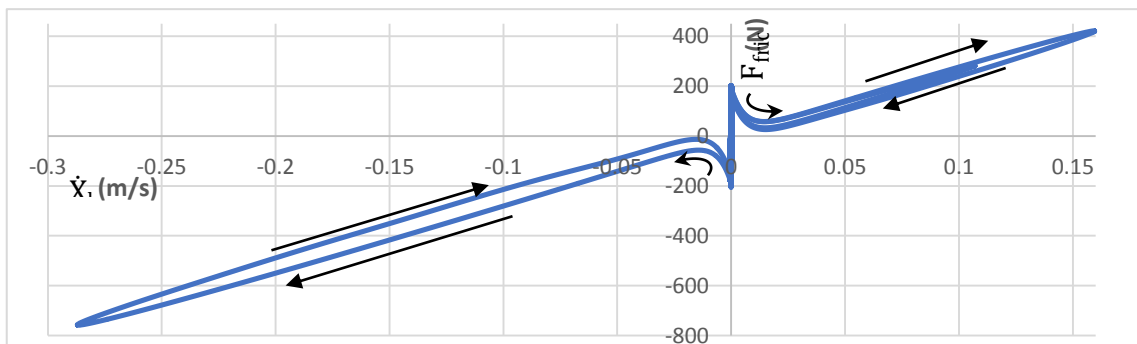Fig. 10 Comparing between $X_w - X_b$ experiment and simulation

Fig.11 Friction as function of the body velocity

6   CONCLUSIONS

Both simulation and experimental results, with several conditions made, showed consistent agreement between experimental and simulation output, which consequently confirmed the feasibility of the new relay model for the passive suspension system that

considered taking into account the actual configuration of test rig system. This model subsequently implements the nonlinearity friction forces that effects on the body linear bearings, is quite accurate and usefulness. The nonlinear friction model captures most of the friction behavior that has been observed experimentally such as stiction region, stribeck effects, the Colombo and viscous frictions that specifically responsible for causing the high relatively difference between the wheel and body travels at the begging test time and so on. In addition, the nonlinear hydraulic actuator, and the dynamic equation of servovalve, models are moderately precise and practicality. The PI control is suggested, successfully derived the hydraulic actuator to valid the control strategy. Even though we are studying and implementing the friction force within the quarter car model, the effecting in real word is so tiny, as consequence to variations into step inputs, still that is vital to open the door for rethinking to consider friction with a quarter, half, and full vehicle models. In addition, this study help to encourage the researchers to implement sliding contact for SS & VD with chassis, which directly be influenced the vehicle stability and road handling. For future work, this is might be good to install an active actuator instated of the passive one, monitoring and using the contact patch load as feedback control signal it was available in our test rig, in order to study system response.

APPENDIX: SYSTEM EQUATIONS

A. Road simulator

Considering Fig. 2, the test rig and road simulator schematic diagram, the spool valve displacement x_{sr} is related to the voltage input u_r by first order system as given by:

$$\dot{x}_{sr} = \frac{1}{\tau_r}(u_r - x_{sr})$$

Where, $\tau_r(s)$ is time servovalve constant, u_r, is servovalve control, x_{sr} (m), is the spool servovalve displacement and $\dot{x}_{sr}$ (m/s), is spool velocity.

The analysis of hydraulic actuator flowrates equation is displayed in two cases as following:

Case 1: If $x_{sr} \geq 0$ when extending, it should check the sign of pressure or pressure differences under square root of the actuator flow rate equation.

if $P_{sr} - P_{1r} \geq 0$

$$Q_{1r} = K_{fr} \, x_{sr}\sqrt{P_{sr} - P_{1r}}$$

if $P_{sr} - P_{1r} < 0$

$$Q_{1r} = -K_{fr} \, x_{sr}\sqrt{P_{1r} - P_{sr}}$$

if $P_{2r} \geq 0$

$$Q_{2r} = K_{fr} \, x_{sr}\sqrt{P_{2r}}$$

if $P_{2r} < 0$

$$Q_{2r} = -K_{fr} \, x_{sr}\sqrt{-P_{2r}}$$

Case 2: If $x_{sr} < 0$ when retracting,

if $P_{sr} - P_{2r} \geq 0$

$$Q_{2r} = K_{fr} \, x_{sr}\sqrt{P_{sr} - P_{2r}}$$

if $P_{sr} - P_{2r} < 0$

$$Q_{2r} = -K_{fr} \, x_{sr}\sqrt{P_{2r} - P_{sr}}$$

if $P_{1r} \geq 0$

$$Q_{1r} = K_{fr} \, x_{sr}\sqrt{P_{1r}}$$

if $P_{1r} < 0$

$$Q_{1r} = -K_{fr}\, x_{sr}\sqrt{-P_{1r}}$$

The actuator flow rate equations, including compressibility and cross-line leakage effects for both sides, may be written as:

$$\frac{V_{1r}}{\beta_r}\, \dot{P}_{1r} = Q_{1r} - A_{1r}\dot{X}_r - \frac{(P_{1r}-P_{2r})}{R_{ir}}$$

$$\frac{V_{2r}}{\beta_r}\, \dot{P}_{2r} = A_{2r}\dot{X}_r + \frac{(P_{1r}-P_{2r})}{R_{ir}} - Q_{2r}$$

$$V_{1r} = V_{1r0} + A_{1r}X_r \tag{17}$$

$$V_{2r} = V_{2r0} - A_{2r}X_r \tag{18}$$

In addition, the Newton second law for tyre mass is,

$$\ddot{X}_r M_r = (P_{1r}A_{1r} - P_{2r}A_{2r} - B_{vr}\dot{X}_r - k_t(X_r - X_w) - B_t(\dot{X}_r - \dot{X}_w) - M_T * g$$

Where, M_r is tyre mass, the displacements of tyre and wheel are X_r , X_w respectively, the velocity of tyre and wheel are $\dot{X}_r, \dot{X}_w$ respectively, $\ddot{X}_r$ is the acceleration of tyre mass, g, is a ground acceleration.

The controller be suggested, is

$$u_r = K_p * e + K_i * e * Ts \qquad \text{[PI controller]}$$

$$e = X_{rd} - X_{rf}$$

Where, u_r, is servovalve control, K_p, is the proportional gain, K_i is the integral gain, e, is the error, Ts (s), time interval, X_{rd} & $X_{rf,}$ (m), are the desired and measured road displacements respectively.

Note: The inputs to the system allows moving the piston of the actuator to mid-point by ramp input and increases or decreases by amplitude values as step input.

B. Account the normal force

Fig.3 be showed the free body diagram of test rig, the friction force acts as an internal force in the tangential direction of the contacting surfaces. Therefore, the inclination position of viscous damper and stiffness spring (VDSS) and the type of inputs to the system will be a help to generate the kinematic bearings body friction relatively to this normal force component, which is conducted by the flowing analysis:

$$F = k_s * (X_w - X_b) + b_d * (\dot{X}_w - \dot{X}_b)/\sin(\theta \mp \Delta\theta) \tag{19}$$

$$F_{nb} = F * \cos(\theta \mp \Delta\theta) \tag{20}$$

$$F_{nb} = k_s * (X_w - X_b) + b_d * (\dot{X}_w - \dot{X}_b)/\tan(\theta \mp \Delta\theta) \tag{21}$$

$$F_{fric} = \mu * F_{nb} \tag{22}$$

Where F_{fric}, is the kinematic sliding frictions, μ is the coefficient of lubricant friction, F_{nb}, is the body normal force component and F is VDSS force.

While the dynamical construction linkage angle is changed by $\mp\Delta\theta$ therefore, we ought to find $\Delta\theta$.

From engineering geometry, we can find:

$$\frac{L_d - \Delta L_d}{\sin(\theta)} = \frac{X_w - X_b}{\sin(\Delta\theta)}$$

$$\sin(\theta) = \frac{\Delta L_d}{X_w - X_b} \qquad \rightarrow \qquad \Delta L_d = (X_w - X_b) * \sin(\theta) \text{ , } \Delta L_d \text{, is the dynamically change in VDSS}$$

length.

Then,

$$\frac{L_d - (X_w - X_b) * \sin(\theta)}{\cos(\theta)} = \frac{X_w - X_b}{\sin(\Delta\theta)} \quad \rightarrow \quad \sin(\Delta\theta) = \frac{(X_w - X_b) * \sin(\theta)}{L_d - (X_w - X_b) * \sin(\theta)}$$

$$\sin \Delta\theta = \frac{(X_w - X_b) * \sin(\theta)}{L_d - (X_w - X_b) * \sin(\theta)}$$

$$\Delta\theta = \sin^{-1}\left[\frac{(X_w - X_b) * \sin(\theta)}{L_d - (X_w - X_b) * \sin(\theta)}\right]$$

References:

Alleyne, A. and Hedrick, J. K. 1995. Nonlinear adaptive control of active suspensions. *IEEE transactions on control systems technology* 3(1), pp. 94-101.

Armstrong-Hélouvry, B. et al. 1994. A survey of models, analysis tools and compensation methods for the control of machines with friction. *Automatica* 30(7), pp. 1083-1138.

Bliman, P. 1992. Mathematical study of the Dahl's friction model. *European Journal of Mechanics, A/Solids* 11(6), pp. 835-848.

Buckner, G. et al. 2015. Intelligent estimation of system parameters for active vehicle suspension control. *CEM Publications*.

FitzSimons, P. M. and Palazzolo, J. J. 1996. Part I: Modeling of a One-Degree-of-Freedom Active Hydraulic Mount. *Journal of Dynamic Systems, Measurement, and Control* 118(3), pp. 439-442.

Hanafi, D. et al. eds. 2009. *Intelligent system identification for an axis of car passive suspension system using real data*. Mechatronics and its Applications, 2009. ISMA'09. 6th International Symposium on. IEEE.

Hardier, G. ed. 1998. *Recurrent RBF networks for suspension system modeling and wear diagnosis of a damper*. Neural Networks Proceedings, 1998. IEEE World Congress on Computational Intelligence. The 1998 IEEE International Joint Conference on. IEEE.

Hedrick, J. and Butsuen, T. 1990. Invariant properties of automotive suspensions. *Proceedings of the Institution of Mechanical Engineers, Part D: Journal of Automobile Engineering* 204(1), pp. 21-27.

Hrovat, D. 1997. Survey of advanced suspension developments and related optimal control applications. *Automatica* 33(10), pp. 1781-1817.

Jamei, M. et al. eds. 2000. *Fuzzy Based Controller of A Nonlinear Quarter Car Suspension System*. Student Seminar in Europe, Manchester, UK.

Karnopp, D. 1985. Computer simulation of stick-slip friction in mechanical dynamic systems. *Journal of dynamic systems, measurement, and control* 107(1), pp. 100-103.

Kirk, D. d. E. Optimal Control Theory. An Introduction. 1970. *Prentice-Hall, Englewood Cliffs, New Jersey)* 3, pp. 417-442.

Maneetham, D. and Afzulpurkar, N. 2010. Modeling, simulation and control of high speed nonlinear hydraulic servo system. *Journal of Automation Mobile Robotics and Intelligent Systems* 4, pp. 94-103.

Merritt, H. E. 1967. *Hydraulic control systems*. John Wiley & Sons. pp. 112-118.

Pathare, Y. S. 2014. Design and Development of Quarter Car Suspension Test Rig Model and It's Simulation. *International Journal of Innovative Research and Development|| ISSN 2278–0211* 3(2).

Surawattanawan, P. 2000. *The influence of hydraulic system dynamics on the behaviour of a vehicle active suspension.* PhD Thesis, , Cardiff University.

Tan, H.-S. and Bradshaw, T. eds. 1997. *Model identification of an automotive hydraulic active suspension system*. American Control Conference, 1997. Proceedings of the 1997. IEEE.

Watton, J. 2007. *Modelling, monitoring and diagnostic techniques for fluid power systems*. Springer Science & Business Media.

Watton, J. 2009. *Fundamentals of fluid power control*. Cambridge University Press.

Westwick, D. T. et al. eds. 1999. *Nonlinear identification of automobile vibration dynamics*. Proc. of the 7th Mediterrean Conference on Control and Automation, Israel*.

Wong, J. Y. 2001. *Theory of ground vehicles*. John Wiley & Sons.